DO CARDIAC ANEURYSMS BLOW OUT?

DANIEL K. BOGEN AND THOMAS A. MCMAHON, *Division of Applied Sciences, Harvard University, Cambridge, Massachusetts 02138 U.S.A.*

ABSTRACT The possibility is suggested that cardiac aneurysms are formed when an infarcted region of the ventricular wall becomes elastically unstable and "blows out." The consequence of such a blowout could be a large saccular aneurysm or even cardiac rupture. We use a nonlinear stress-strain relation capable of describing both the passive and active myocardial wall to examine this possibility in terms of large-deformation membrane theory. Ventricular infarcts made of a material having physical properties like rubber would be expected to blow out, but those made of passive myocardium would not.

INTRODUCTION

A possible sequel to infarction of the left ventricle is the development of a saccular aneurysm of noncontracting myocardium. The aneurysm can develop rapidly, in the course of a few hours after the infarct, or it may require several days. In exceptional circumstances an aneurysm of the left ventricle may rupture abruptly. This paper considers the theoretical question of whether or not the rupture of a ventricular aneurysm, or even the original development of its saccular form, can be understood as an elastic instability analogous to the blowout of an automobile tire.

Relatively little is presently known about the formation and rupture of cardiac aneurysms. A previous approximate mechanical analysis of aneurysms (Lowe and Love, 1948) indicated that aneurysmal bulging was consistent with altered elastic properties of that region; but more accurate analyses, as well as consideration of the blowout question, have not yet received attention.

The phenomenon of elastic instability, or blowout, is familiar to anyone who has inflated an ordinary synthetic rubber balloon. The initial inflation is accomplished with a good deal of effort, requiring progressively increasing pressures. However, beyond a certain point, continued inflation requires considerably less effort and in fact smaller pressures than those required initially. This peculiar characteristic of increasing volume with decreasing pressures is the essence of elastic instability and is responsible for the fact that when such a balloon is connected to a large constant-pressure reservoir, increasing reservoir pressures correspond to continuously increasing balloon volumes until a critical pressure is reached, when a sudden discontinuous increase in balloon volume is seen. In some cases, this increase in balloon volume may be indefinite, terminated only by balloon rupture.

There is no reason to expect a priori that a region of the left ventricular wall with altered mechanical properties would or would not blow out like a rubber balloon. Of all the parameters of the problem that might determine the criteria for blowout, including the size and stiffness of the infarcted region, and the nature of the interaction between the infarcted region and the surrounding viable tissue, it turns out that a single parameter describing the nonlinearity of the stress-strain (constitutive) relation in the infarcted region determines

whether blowout occurs or not. In what follows, this simple result is developed by considering several different idealized geometries, each representative of some special feature of the aneurysm problem. We begin with a simple thin-walled sphere, for which a closed-form solution exists relating pressure and volume, even when the wall of the sphere is made of a realistically nonlinear material. Then we consider a membrane of this material bulging through a circular hole in a rigid plane. Later, the membrane is generalized to a spherical cap, which also bulges through a hole, and finally we postulate the inflation of two such caps, joined at their edges by suitable matching conditions. The result from each problem is the same, which allows the blowout criterion for nonlinear materials typical of the myocardial wall to be stated in fairly general terms.

METHODS

Spherical Rubber Balloons

The pressure-volume behavior of spherical rubber balloons is well understood in terms of large deformation elastic theory. Both Alexander (1971) and Ogden (1972) have given solutions for the inflation of a rubber balloon. Alexander approached the problem by employing the method of stationary total potential energy. This approach is particularly interesting because it reveals the stability condition of the balloon at different points of inflation. A state of local minimum total potential energy is one of stable equilibrium; a state of local maximum total potential energy is one of unstable equilibrium; and an inflection point in total potential energy indicates neutral stability. By determining the nature of the stationarity in total potential energy, Alexander was able to determine the nature of balloon stability. His results are displayed in Fig. 1. Passing from one stable equilibrium position to another at the same pressure requires surmounting an energy barrier. This energy barrier takes the form of a local energy maximum which separates the local minima of the stable equilibrium positions. Starting from zero pressure, the energy barrier decreases with continued inflation until the blowout pressure (point 1) is reached. This is a position of neutral equilibrium and no energy barrier lies between it and the position of stable equilibrium (point 2) at much larger volume.

Ogden (1972) used a different scheme of analysis to obtain an equivalent result. Although Ogden was especially interested in rubber balloons, his analysis is applicable to any material with a strain energy function of the form:

$$\Phi = \mu_p \left(\lambda_1^{k_p} + \lambda_2^{k_p} + \lambda_3^{k_p} - 3 \right) \Big/ k_p. \tag{1}$$

Here, Φ is the strain energy density; λ_1, λ_2, and λ_3 are the principal extensions; and μ_p and k_p are

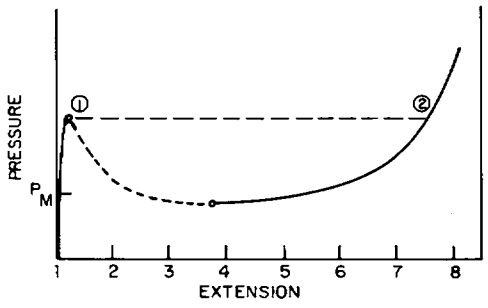

FIGURE 1 Pressure-extension relation in a spherical rubber balloon, adapted from Alexander (1971). Here extension denotes the ratio of the radius of the inflated balloon to the radius of the initial uninflated balloon. Note that there exist two points, (1) and (2), at the same pressure.

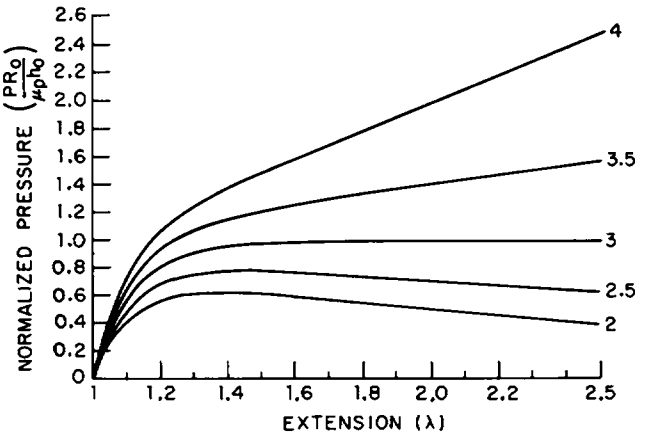

FIGURE 2 Pressure-extension relations in spherical membranes with power-law constitutive properties, with power-law constant from 2.0 to 4.0. These relations are described also by Eq. 2.

material constants (the exponent p refers to the power-law form). Rubber is well described for moderate extensions by Eq. 1 with the power-law constant $k_p = 2$. A simple kinetic molecular theory, assuming that rubber is composed of long chain hydrocarbon molecules free to rotate around the carbon links, may be used to derive Eq. 1 with $k_p = 2$ (Treloar, 1975). For very large extensions, additional power-law terms must be added to the strain energy function (Ogden, 1972). Fortunately for the purposes of this paper, there is also strong evidence that passive myocardium, and therefore the wall material included in a fresh infarct, is well described for extensions in the physiological range by Eq. 1, provided that k_p is taken in the neighborhood of 18. (Bogen, 1977; Laird, 1976; Janz and Waldron, 1978). No derivation of the k_p for passive myocardium from basic principles has yet been given.

When Eq. 1 is employed as the constitutive relation, the inflation pressure, P, is given in terms of the initial (zero-pressure) thickness, h_0, the initial radius, R_0, and the circumferential extension, λ, as:

$$P = \frac{2h_0\mu_p}{R_0}\left(\lambda^{k_p-3} - \lambda^{-2k_p-3}\right). \tag{2}$$

This result, along with the equivalent pressure-volume relation, is derived in Appendix I, and plotted for several values of k_p in Fig. 2.

It is readily apparent that a maximum exists in the pressure-extension curve for small values of k_p but not for large ones. The reason for this is seen if one considers the equation of equilibrium between wall stress, σ, and pressure, P (Laplace's law):

$$P = 2\sigma h/R. \tag{3}$$

Since R varies with the extension λ, and h varies as λ^{-2} due to incompressibility, it is clear that unless σ varies as λ^q, where $q \geq 3$, P will decrease at higher inflations. Indeed, by differentiating the pressure-extension expression with respect to extension, and setting the derivative equal to zero, Ogden (1972) was able to show that a local pressure maximum exists for $-3/2 < k_p < 3$. Hence the elastic instability of the rubber balloon, with $k_p = 2$, is predicted. Understanding the behavior of the balloon at inflations beyond the pressure maximum, however, requires a constitutive relation which is more accurate at larger extensions.

The conclusion of the above analysis is that a thin-walled sphere made of passive myocardium, described by Eqs. 1 and 2 with $k_p = 18$, is not subject to elastic blowout, in contrast to the rubber balloon.

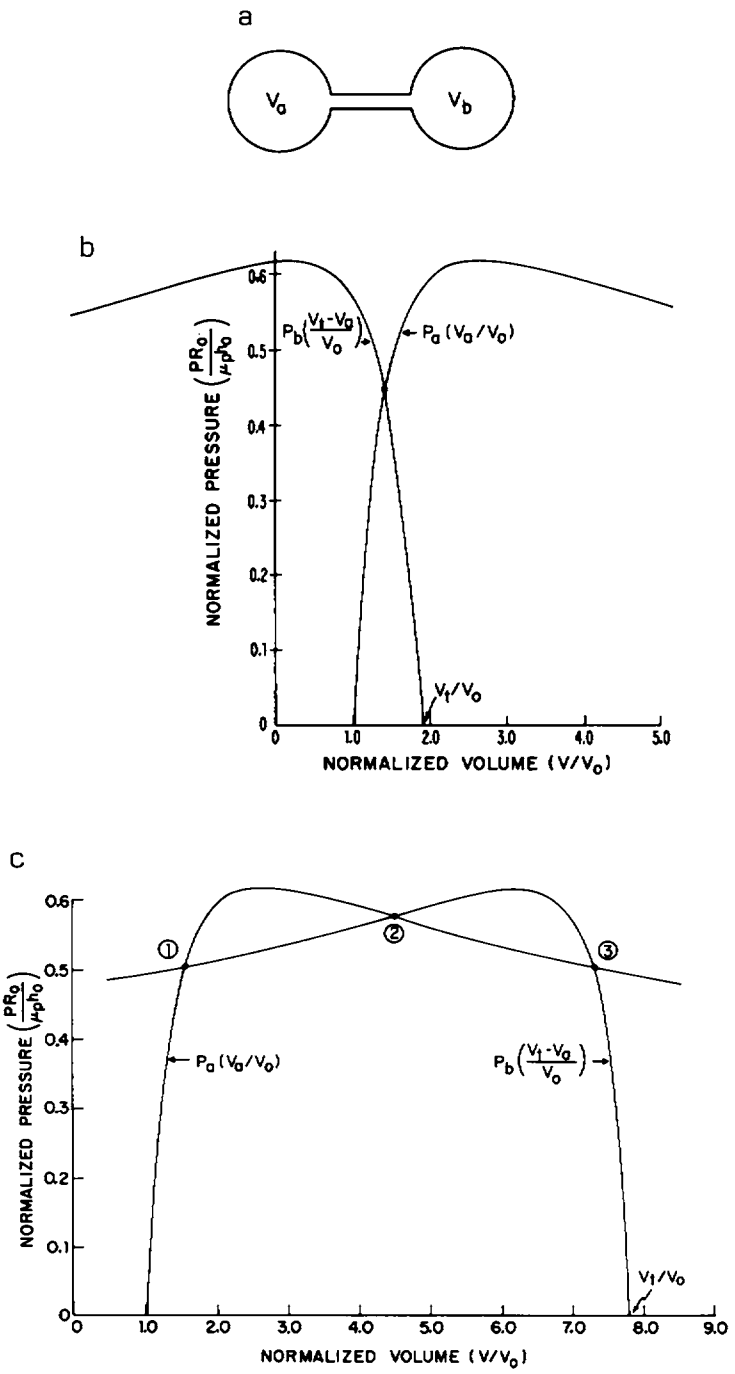

FIGURE 3 (*a*) Simple system with two communicating spherical (balloon) compliance chambers, V_a and V_b. (*b*) Pressure-volume relations, P_a and P_b, for individual balloons in the two balloon system portrayed in Fig. 3 *a*, normalized by the zero-pressure volume V_0. Total volume for the whole system is V_t. Pressure-volume relations are also given by Eq. 4. (*c*) Pressure-volume relations for individual balloons in two balloon system in which V_t is such that more than one equilibrium configuration exists.

The Aneurysmal Heart in Isovolumic Systole

Until this point the aneurysm has been considered in isolation. We now introduce the simplest possible coupling between the aneurysm and the ventricle. Suppose the remaining viable heart and the aneurysm are represented by two separate compliant spheres, *a* and *b*, connected by a rigid tube (Fig. 3 *a*). The pressure-volume relations for the two spheres are given by $P_a(V_a)$ and $P_b(V_b)$. If the separate pressure-volume curves should have pressure maxima, these will be denoted by P_a^* and P_b^*. The pressure-volume relation for the whole two- component system is given by $P_t(V_t) = P_t(V_a + V_b)$.

In general, the blowout pressure for a multicomponent system occurs at the smallest of the subcomponent blowout pressures. A corollary to this statement is that in a multicomponent system a particular component is not subject to blowout if there exists another component with a lesser blowout pressure. This assumes that each component has a pressure-volume curve with at most one maximum and no minimum.

An interesting feature of a multicomponent compliant system is that at a given total system volume there may be more than one possible equilibrium configuration. This is seen as follows for a two-component system.

If the total volume is given by V_t, then at equilibrium $P_a(V_a) = P_b(V_b)$, where $V_a + V_b = V_t$; or equivalently, the system is in equilibrium when $P_a(V_a) = P_b(V_t - V_a)$. This last equation is portrayed in Fig. 3 *b*, for the special case of two identical balloons whose individual pressure-extension relations are given by (2) with $k_p = 2$. The normalized pressure-volume relation in each balloon is therefore given by:

$$\frac{PR_0}{2\mu_p h_0} = \left(\frac{V}{V_0}\right)^{-1/3} - \left(\frac{V}{V_0}\right)^{-7/3}, \tag{4}$$

where V_0 is the zero-pressure volume of a single balloon. The intersection of the curves indicates the single stable equilibrium position possible for the given V_t. However, for a larger V_t, the situation is as in Fig. 3 *c*, with three points of intersection between the two curves $P_a(V_a)$ and $P_b(V_t - V_a)$. Points 1 and 3 are points of stable equilibrium. This may be demonstrated as follows. An externally applied perturbation in V_a, moving the state point to the right of point 3, leads to an increase in P_a above that in P_b. Therefore, the volume of sphere *a* tends to drop when the perturbation is released, restoring the system to the equilibrium point. Point 2 is unstable, however: a positive perturbation in V_a (to the right) causes P_b to exceed P_a, leading to a further increase in V_a when the perturbation is released.

Suppose the two identical balloons were inflated separately to the same volume, then joined together by the pipe shown in Fig. 3 *a*. The total volume of the two balloons would be $V_t = V_a + V_b = 2V_a$, provided that the balloons remained at equal volume after they were in communication. In Fig. 4, the normalized pressure vs. total volume under these assumptions is shown as line *ii*.

In actual fact, the volumes of the two $k_p = 2$ balloons would remain equal after they were in communication only on the ascending part of curve *ii*. Once the total volume rises above the maximum-pressure point, there exists for every total volume another, lower-pressure solution, corresponding to points 1 or 3 in Fig. 3 *c*, where most of the volume is present in only one of the balloons. Curve *iii* in Fig. 4 shows this lower-pressure, stable solution as a function of V_t. It was obtained by numerically solving the equations $P = P(V_a) = P(V_b)$; $V_t = V_a + V_b$, and $P_a = P_b(V_t - V_a)$. The pressure-volume curve for a single balloon alone is shown as line *i*, for comparison.

The overall conclusion is that elastic instability still requires a maximum on the aneurysmal pressure-volume curve such as that shown in line *i*, as discussed earlier. But when a scheme such as that shown in Fig. 3 *a* represents the aneurysmal heart contracting in isovolumic systole, the ventricular pressure is now allowed to reach the pressure maximum of curve *i* without the consequence of the aneurysm blowing out to infinite volume. This is because the heart and the aneurysm share a finite volume, and therefore the aneurysm cannot grow to an indefinitely large size.

The Isolated Aneurysm

The large-deformation problem for a sphere, while instructive because of its closed-form result, is not a reasonable point at which to leave the question of the elastic stability of cardiac aneurysms. A geometry

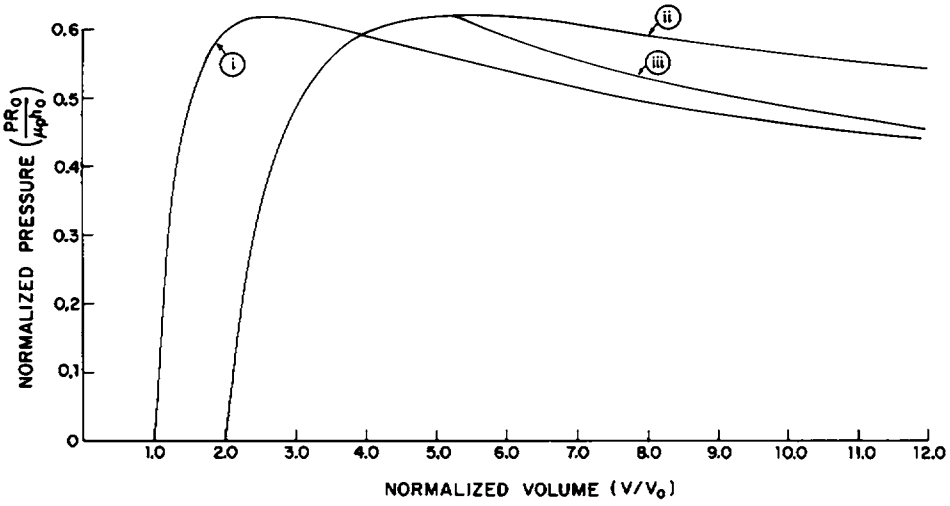

FIGURE 4 Pressure-volume relation for the whole two balloon system portrayed in Fig. 3 *a*. Curve *i* is the pressure-volume relation for a single balloon. Curve *ii* describes the hypothetical system pressure-volume curve that would occur if the balloons always were of equal volume. Curve *iii* is the actual system pressure-volume curve which departs from curve *ii* because the total volume actually divides unequally between two balloons.

somewhat more representative of the infarcted region is that of a dome-like membrane bulging through a circular hole in a rigid plane.

A cylindrical polar coordinate system for the undeformed membrane (isolated aneurysm) is shown in Fig. 5 *a*. When zero pressure difference acts across the membrane, its (undeformed) shape is assumed to be that of a spherical cap. The position of a point B_0 is described by (ρ, θ, x_3), where the x_3 axis lies along the axis of revolution of the shell. Under axisymmetric deformation, the point B_0 is carried to the point B described by the coordinates (r, θ, y_3) on the deformed shell.

In this system, curves of constant θ on the shell surface describe meridian curves on the shell. Next, a curvilinear surface coordinate system (η, θ) for the undeformed shell will be introduced. The distance of B_0 from a reference point A_0 along the meridian curve containing B_0 and A_0 is η. In the problems considered here the deformed shells have dome-like configurations whose apices intersect the y_3 axis. In

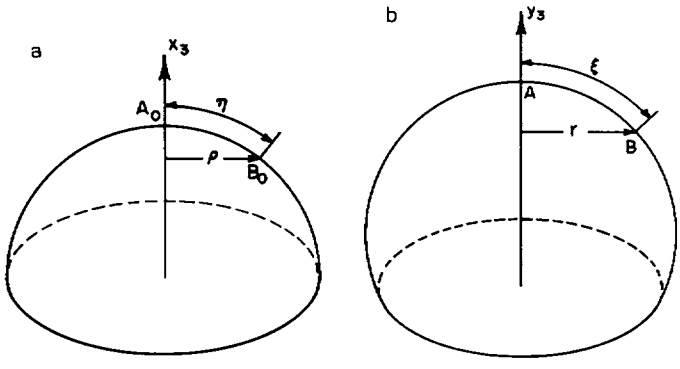

FIGURE 5 (*a*) Cylindrical coordinate system (ρ,θ,x_3) of the undeformed shell. The angular coordinate θ is not shown here because of the axial symmetry of the problem. (*b*) Cylindrical coordinate system (r,θ,y_3) of the deformed shell.

this case, ξ is the distance from the apex, A, to point B along the meridian. Thus, a curvilinear surface coordinate system (ξ, θ) may be introduced for the deformed shell. The deformed coordinate system is displayed in Fig. 5 *b*.

A brief derivation of the equations of equilibrium and geometrical constraint for the deformed membrane appears in Appendix II. Because of the symmetry of the problem, with lines of principal curvature, principal stress, and principal strain all following lines of longitude and latitude of the membrane, the equations of equilibrium reduce to a simple form. Deformation is described in terms of the principal extensions, λ_1 and λ_2, which lie in the longitudinal and latitudinal directions, respectively. The longitudinal extension, λ_1, is the ratio of the length of an infinitesimal longitudinal segment in the deformed, as compared to the undeformed, shell, and hence $\lambda_1 = d\xi/d\eta$. Because of symmetry, λ_1 is a function of ξ only. Similarly, λ_2 is the ratio of deformed to undeformed segment lengths along a line of latitude, and hence $\lambda_2 = r/\rho$. Due to axial symmetry, λ_2 is a function of ξ only.

RESULTS

Initially Flat Circular Membrane

The solution of the equations of Appendix II for the inflation of an initially flat, circular, $k_p = 2$ membrane was first presented by Green and Adkins (1960), employing a shooting method for the numerical integrations. For the purposes of this paper, where the initial geometry is nonplanar and where an additional task (described later) will be the matching of two shells together at their margins, it was necessary to employ a method of numerical integration, the fourth-order Runge-Kutta method, more accurate than that employed by Green and Adkins. Details of the computational procedure are given in Bogen (1977). Once the shape of the membrane was determined for a given inflation pressure, P, the volume enclosed by the deformed membrane and the $y_3 = 0$ plane was calculated. The results were generally presented as normalized pressure, $P\rho_0/\mu_p h_0$, against normalized added volume. Here μ_p is a material constant defined in Eq. 1, h_0 is the initial membrane thickness, and ρ_0 is the radius of the hole through which the membrane bulges.

The first use of the program was a calculation of the inflation curve for the initially flat membrane, shown in Fig. 6 *a*, when the material properties are described by Eq. 1 with $k_p = 2$. The result is identical with that reported by Green and Adkins, and shows a pressure maximum in the neighborhood of $\Delta V/\rho_0^3 = 2$, i.e., when the membrane shape is nearly

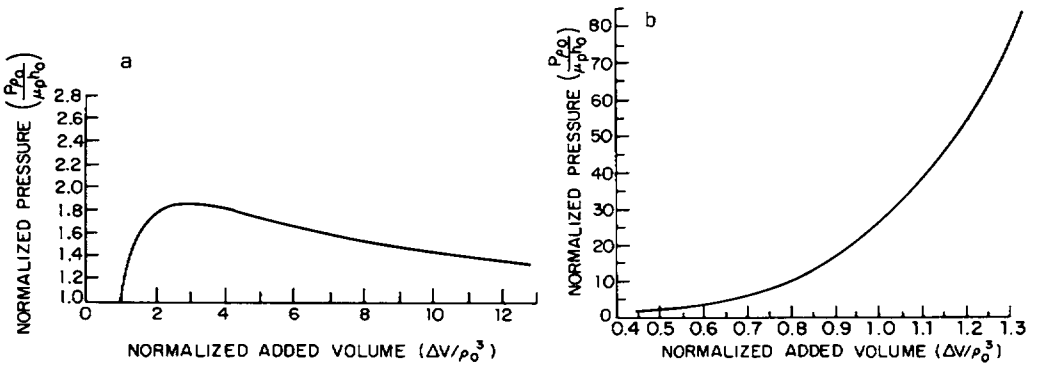

FIGURE 6 (*a*) Pressure-volume relation for the inflation of an initially flat, circular $k_p = 2$ membrane. (*b*) Pressure-volume relation for the inflation of an initally flat, circular $k_p = 18$ membrane. The membrane bulges through a hole of radius ρ_0.

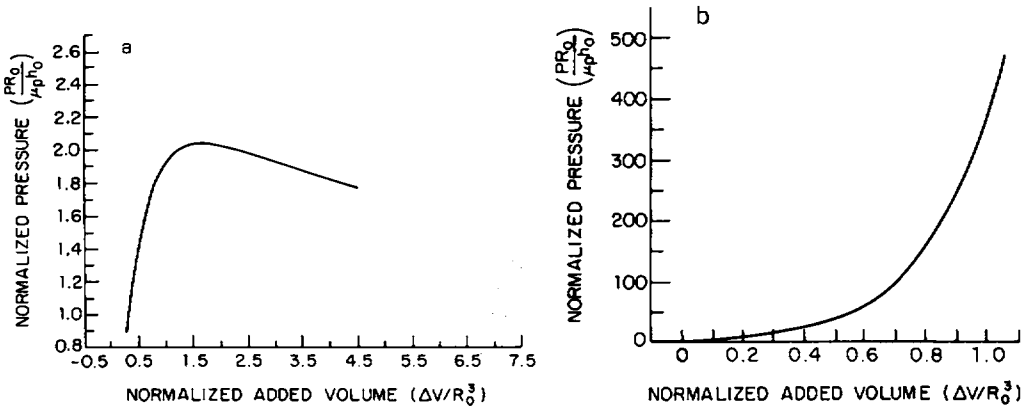

FIGURE 7 (*a*) Pressure-volume relation for the inflation of a $k_p = 2$, 60° half-angle, spherical cap membrane. See Fig. 9 *a* for definition of half-angle. (*b*) Pressure-volume relation for the inflation of a $k_p = 18$, 60° half-angle, spherical cap membrane. The cap bulges through a hole of fixed radius R_0.

hemispherical. The same calculation is repeated in Fig. 6 *b* when $k_p = 18$, and shows a montonically increasing behavior. By the arguments advanced earlier, the myocardial membrane is not subject to elastic blowout.

Spherical Cap Membrane

Since the ventricular aneurysm has a geometry somewhere between that of the sphere and that of the initially flat membrane, it seemed sensible to examine the inflation of a spherical cap, a more realistic case. The results are shown in Figs. 7 *a* and *b* for a spherical cap of half-angle 60°. Not surprisingly, the $k_p = 2$ cap has a pressure maximum and the $k_p = 18$ cap does not. The myocardial aneurysm still appears to be elastically stable.

Can Blowout be Induced by Membrane Edge Conditions?

The potential for elastic blowout in the ventricular aneurysm has not yet been completely eliminated. Until now, the only coupling considered between the aneurysm and the ventricle has been the fact that they share a common fluid volume during isovolumic systole. The possibility remains that the viable myocardium surrounding the aneurysm alters the dimensions of the ring-like junction between the infarcted and the viable myocardium, thereby inducing elastic instability in the aneurysm by some complex mechanism.

To consider this possibility, pressure-volume curves were determined for various caps and for the initially flat membrane when the ring was constricted or extended by suddenly changing the diameter of the ring after inflation had begun. The result for a spherical cap of initial half-angle 60° is shown in Fig. 8 *a* for a $k_p = 2$ material. The numbers by each curve show the fraction by which the boundary ring is either constricted ($\lambda_2 < 1$) or extended ($\lambda_2 > 1$) by an outside agency after the inflation has begun. Fig. 8 *b* shows that even if the edge of the myocardial $k_p = 18$ membrane is constricted, the membrane maintains its elastic stability; the pressure-volume curves show no pressure maxima, although constricting the membrane edge does increase the pressure for a given normalized added volume. It is interesting to note that for the $k_p = 2$ membrane (Fig. 8 *a*) constriction of the edge to a

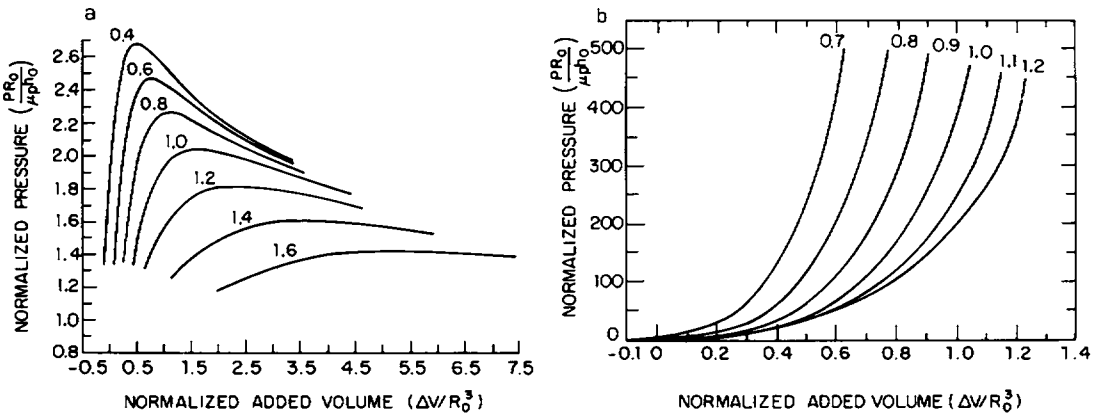

FIGURE 8 (*a*) Pressure-volume relations for the inflation of a $k_p = 2$, 60° half-angle, spherical cap membrane whose edge is extended or constricted by λ_2 from 0.4 to 1.6. (*b*) Pressure-volume relation for the inflation of a $k_p = 18$, 60° half-angle, spherical cap membrane whose edge is extended or constricted by λ_2 from 0.7 to 1.2.

smaller radius increases the blowout pressure but reduces the volume at which blowout occurs.

Two-Material Spherical Elastic Membrane

It is not possible, of course, to know a priori whether the ring separating the viable myocardium from the aneurysmal region constricts or dilates during systole. Insight into this question may be obtained by considering the inflation of an initially spherical membrane composed of two different materials arranged as in Fig. 9 *a*. This problem was considered as the inflation of two separate spherical caps under the same pressure subject to their being matched by the appropriate boundary conditions at their edges.

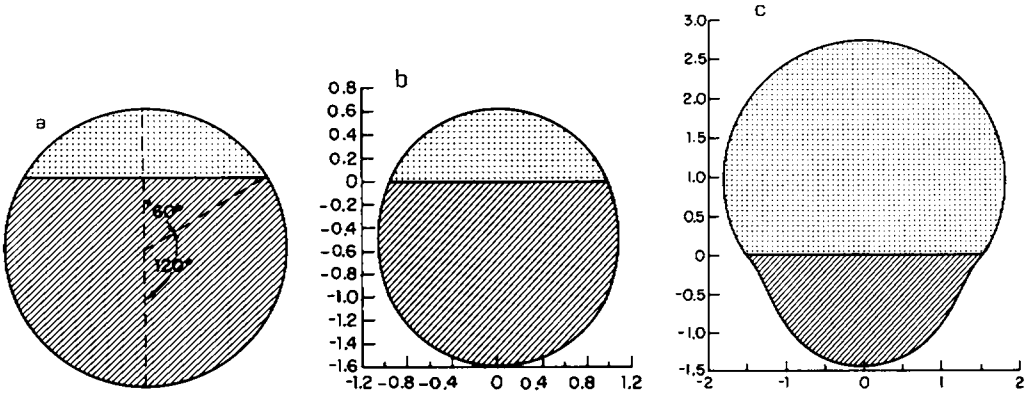

FIGURE 9 (*a*) Initial configuration (zero pressure) of a two-material spherical membrane. The upper cap, which is half-thickness, has a half-angle of 60°, leaving the lower full-thickness cap to occupy a half-angle of 120°. (*b*) Deformed configuration of inflated balloon. Dot shading indicates single thickness region; diagonal shading indicates double thickness. (*c*) Deformed configuration of inflated two-material balloon. Figs. 9 *b* and *c* are two separate shapes at the same pressure. This is the blowout phenomenon, illustrated schematically in Fig. 1.

There are two boundary conditions. First, the two caps must have circular edges of the same size. This is equivalent to stating that λ_2 is continuous at the boundary between the two materials. Secondly, the stress resultant in the longitudinal direction must be continuous in order that equilibrium at the boundary be satisfied. Since the inflation pressure of both caps is the same, this is equivalent to stating that the longitudinal slope, dy/dr, must be continuous at the boundary.

The inflation of such an inhomogeneous sphere is a two-point boundary value problem. In this instance, values of λ at the two apices must be chosen as initial conditions, such that the two boundary conditions of continuous λ_2 and continuous slope dy/dr are satisfied. In actual practice the correct apical λ's were determined by a combination of trial and error and the Newton-Raphson method.

As an example of a use of the method, take the specific case of a spherical rubber ballon which is specially constructed so that a region covering 25% of the surface of the undeformed membrane has an undeformed thickness one-half the thickness of the rest of the balloon. It would be expected that this thin region would bulge substantially when the balloon is inflated.

This problem was solved by considering the rubber balloon as a $k_p = 2$ material and matching the solutions for a 60° half-thickness cap and a 120° full-thickness cap, as shown in Fig. 9 *a*. The $k_p = 2$ description of rubber is not precisely correct but is considered adequate for the range of extensions encountered in the actual solution of this problem. One case in particular will be presented here: that in which the nondimensionalized pressure of the balloon $PR_0/\mu_p h_0 = 0.55$, where h_0 is the thickness of the thicker portion of the balloon. Actually, two solutions at this pressure were found. The balloon shapes predicted by these solutions are displayed in Figs. 9 *b* and *c*.

The predictions in Figs. 9 *b* and *c* can be corroborated experimentally. Two approximately spherical rubber balloons were placed one inside the other so that they formed a double thickness balloon. A circular region was cut out of the outer balloon so that approximately 25% of the surface of the composite balloon was only of single thickness. The edges of the cut balloon were then secured to the inner balloon with rubber cement. The composite balloon was attached to a pressure reservoir, and the inflation pressure was slowly increased. At a critical level of pressure, the thinned region abruptly bulged out. One particular inflation of this composite balloon is shown in Fig. 10, a photograph that looks much like the theoretical shape for the same problem shown in Fig. 9 *c*.

Contraction of the Viable Myocardium

Strong evidence exists for taking the constitutive relation (1) with $k_p = 2$ as representative of actively contracting myocardial tissue, provided that the rest length, i.e., the length at which an element of myocardium develops zero tension, is assumed to abruptly decrease when the muscle becomes active (Bogen, 1977). The value for k_p follows from observations by Grimm et al. (1970) that papillary muscle developed tension is essentially linear with extension in the physiological range. This developed tension can therefore be described in terms of neo-Hookean ($k_p = 2$) material properties. The extent of change in sarcomere rest length can be determined from the ventricular muscle data of Spotnitz et al. (1966), and from the papillary muscle measurements of Grimm et al. (1970). Both of these sources show that the ratio of rest length before and after contraction λ_c is about 1.18.

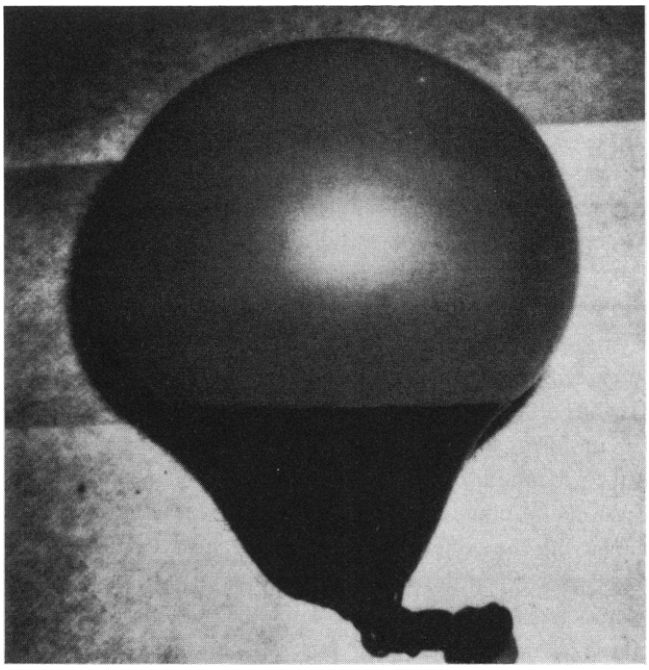

FIGURE 10 Photograph of inflated inhomogeneous rubber balloon. Light region is single thickness rubber; dark region is double thickness.

With the determination of λ_c, all that remains in determining a systolic model of the infarcted ventricle is the determination of the factor $(h_0\mu_p/R_0)$ for the viable myocardium. This was accomplished by selecting $(h_0\mu_p/R_0)$ so that the maximum developed pressure for a noninfarcted spherical ventricle would be 250 mmHg. Details are given in Bogen (1977).

When an initially spherical heart, containing a 25% $k_p = 18$ passive infarct, is allowed to contract to $\lambda_c = 1.18$, the result is as shown in Fig. 11. Figs. 11 *a*, *b*, and *c* show three different total volumes corresponding to inflation pressures of 50, 100, and 150 mmHg, respectively. At

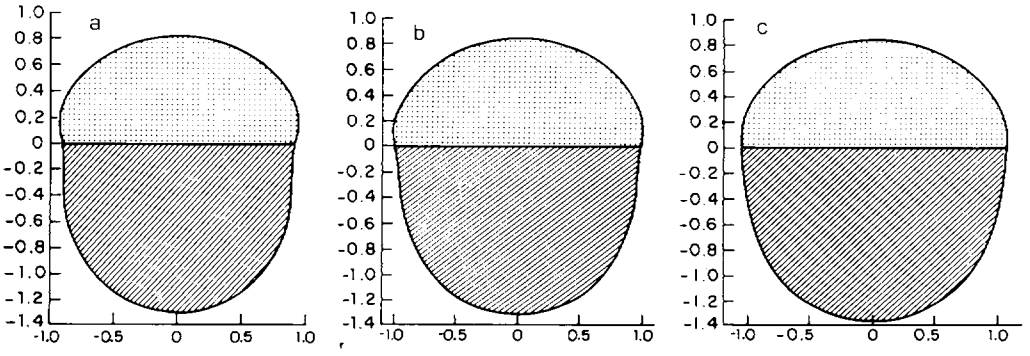

FIGURE 11 (*a–c*) Configuration of an initially spherical ventricle with a 25% (60° half-angle) infarct, at end-systolic pressures of 50, 100, 150 mmHg, respectively. The larger pressures have been obtained by increasing total included volume.

low pressures, the aneurysm bulges somewhat as the viable myocardium contracts, but at high pressures, the whole heart returns toward spherical geometry. There is no tendency for the infarct material to blow out.

DISCUSSION

The failure of the initially flat (Fig. 6 *b*) and spherical cap (Fig. 7 *b*) $k_p = 18$ membranes to blow out is not unexpected in light of the stability of the $k_p = 18$ sphere. It is likely that very large inflations of axisymmetric membranes, regardless of their initial geometries, result in deformed geometries which asymptotically approach that of a sphere. This has been shown to be the case for axisymmetric Mooney-material balloons by Wu (1972), and for axisymmetric Mooney-material membranes with fixed edges by Wu and Perng (1972).

If very large inflations of a membrane did result in an (almost) spherical shape, then there would be virtually uniform stresses and extensions over the surface of the deformed membrane, except for a boundary layer near the membrane edge. In this case the pressure-volume relation of the membrane at large inflations would be essentially that of an initially spherical membrane having the same constitutive properties.

Since a $k_p = 2$ spherical balloon shows decreasing pressure with increasing volume at higher inflations, any axisymmetric $k_p = 2$ membrane would be expected to show decreasing pressure with increasing volume at high enough inflations. This implies that any axisymmetric $k_p = 2$ membrane has a local pressure maximum and is subject to elastic blowout. On the other hand, since the $k_p = 18$ sphere shows increasing pressure with increasing volume at high inflations, any axisymmetric membrane eventually would be expected to show increasing pressure with increasing volume at high enough inflations. Therefore, if a $k_p = 18$ axisymmetric membrane does have a local pressure maximum, it must also have a local pressure minimum. In none of the geometries considered in this paper was this seen. Therefore, elastic blowout in a $k_p = 18$ aneurysm appears unlikely.

If the mechanism of aneurysm formation and rupture is not elastic instability, then what is it? Degenerative changes in the ventricular wall, including muscle cell necrosis and edema, almost certainly change not only the elastic but the plastic properties of the tissues in the critical post-infarction period. A great deal more needs to be discovered about the physical nature of these degenerative changes before the mechanical principles behind the formation of ventricular aneurysms become clear.

APPENDIX I

Ogden's Derivation of the Pressure-Extension Relation of a Spherical Balloon

Given a strain energy function of the form

$$\Phi = \mu_p(\lambda_1^{k_p} + \lambda_2^{k_p} + \lambda_3^{k_p} - 3)/k_p,$$

where λ_i are the principal extensions and μ_p and k_p are constants, the stress-strain relation of a membrane under equibiaxial tension, assuming plane-stress and incompressibility, is

$$\sigma = \mu_p(\lambda^{k_p} - \lambda^{-2k_p}),$$

where σ is Cauchy stress (force/deformed cross-sectional area) and λ is the surface extension (stretched

length/unstretched length.). Along with this constitutive relation three more equations are needed to describe the mechanics of the spherical membrane. The first is the equation of equilibrium for a thin-walled sphere, $P = 2\sigma h/R$. The second is the equation describing the conservation of wall volume, $4\pi R_0^2 h_0 = 4\pi R^2 h$, where the subscripts 0 refer to the initial unstressed state. The third equation is the definition of extension, $\lambda = R/R_0$. The last two expressions together imply $h = h_0/\lambda^2$. Appropriate manipulation of the equations then gives

$$P = \frac{2\mu_p h_0}{R_0}(\lambda^{k_p-3} - \lambda^{-2k_p-3}).$$

APPENDIX II

The following analysis is a generalization of the work of Green and Adkins (1960) for axially symmetric membranes under pressure loading. The coordinate system shown in Fig. 5 is discussed in the text.

Equilibrium Equations

There are actually three conditions determining equilibrium in the longitudinal, latitudinal, and normal directions. In the longitudinal direction, force equilibrium is established by:

$$d(T_1 r)/d\xi = T_2(dr/d\xi), \tag{II-1}$$

where T_1 and T_2 are the stress resultants or tensions in the longitudinal and latitudinal directions, respectively. Because of symmetry, T_1, T_2, and r are all independent of θ; and for this reason equilibrium in the latitudinal direction is automatically satisfied. Equilibrium in the normal direction is described by

$$\kappa_1 T_1 + \kappa_2 T_2 = P, \tag{II-2}$$

where P is the normal pressure difference across the membrane and κ_1 and κ_2 are the (principal) curvatures in the longitudinal and latitudinal directions, respectively.

Next, two geometrical equations are introduced. The first is one of the Codazzi equations:

$$d(\kappa_2 r)/d\xi = \kappa_1(dr/d\xi). \tag{II-3}$$

(The other Codazzi equation is identically zero.) Eq. II-3, along with the equation for longitudinal curvature,

$$\kappa_1 = -\frac{d^2r/d\xi^2}{[1 - (dr/d\xi)^2]^{1/2}}, \tag{II-4}$$

implies the second of the geometrical equations:

$$\kappa_2 r = \left[1 - \left(\frac{dr}{d\xi}\right)^2\right]^{1/2}. \tag{II-5}$$

Deformation is described in terms of the principal extensions, λ_1 and λ_2, which lie in the longitudinal and latitudinal directions, respectively. Hence $\lambda_1 = d\xi/d\eta$, and $\lambda_2 = r/\rho$.

The principal stresses, σ_1 and σ_2, in the longitudinal and latitudinal directions, are related to λ_1 and λ_2 according a constitutive relation in the Ogden form (Eq. 1), with the assumptions of incompressibility ($\lambda_1\lambda_2\lambda_3 = 1$) and plane stress ($\sigma_3 = 0$). Thus, for a strain energy function with a power of k_p, σ_1 and σ_2 are given by $\sigma_1 = \lambda_1^{k_p} - \lambda_3^{k_p}$, $\sigma_2 = \lambda_2^{k_p} - \lambda_3^{k_p}$. The stress resultants, T_1 and T_2, are related to the stresses by $T_1 = (\lambda_3 h_0)\sigma_1$ and $T_2 = (\lambda_3 h_0)\sigma_2$, where h_0 is the undeformed thickness of the shell. Hence, T_1 and T_2, which enter into the equations of equilibrium, are given by

$$T_1 = (\mu_p h_0)\,[\lambda_3(\lambda_1^{k_p} - \lambda_3^{k_p})]$$

and

$$T_2 = (\mu_p h_0)\,[\lambda_3(\lambda_2^{k_p} - \lambda_3^{k_p})]. \tag{II-6}$$

The governing equations in summary are:

$$\mathrm{d}(T_1 r)/\mathrm{d}\xi = T_2(\mathrm{d}r/\mathrm{d}\xi) \tag{II-7}$$

$$\kappa_1 T_1 + \kappa_2 T_2 = P \tag{II-8}$$

$$\mathrm{d}(\kappa_2 r)/\mathrm{d}\xi = \kappa_1(\mathrm{d}r/\mathrm{d}\xi) \tag{II-9}$$

$$\kappa_2 r = [1 - (\mathrm{d}r/\mathrm{d}\xi)^2]^{1/2} \tag{II-10}$$

$$T_1 = (\mu_p h_0)\,[\lambda_3(\lambda_1^{k_p} - \lambda_3^{k_p})] \tag{II-11}$$

$$T_2 = (\mu_p h_0)\,[\lambda_3(\lambda_2^{k_p} - \lambda_3^{k_p})] \tag{II-12}$$

$$\lambda_1\lambda_2\lambda_3 = 1 \tag{II-13}$$

$$\lambda_1 = \mathrm{d}\xi/\mathrm{d}\eta \tag{II-14}$$

$$\lambda_2 = r/\rho \tag{II-15}$$

The Differential Form of the Membrane Equations

In the preceding set of equations T_1, T_2, κ_1, κ_2, and r are all functions of ξ. To solve these equations, however, it will be more convenient to put them in a form in which the independent variable is η. In addition, it will be helpful to put all the equations in a derivative form. By applying the chain rule to

$$\mathrm{d}T_1/\mathrm{d}\xi = (\mathrm{d}T_1/\mathrm{d}\eta)\,(\mathrm{d}\eta/\mathrm{d}\xi) = (\mathrm{d}T_1/\mathrm{d}\eta)\,(1/\lambda_1)$$

and to

$$\mathrm{d}r/\mathrm{d}\xi = (\mathrm{d}r/\mathrm{d}\eta)\,(\mathrm{d}\eta/\mathrm{d}\xi) = (\mathrm{d}r/\mathrm{d}\eta)\,(1/\lambda_1),$$

Eq. II-7 becomes

$$\mathrm{d}T_1/\mathrm{d}\eta = -\,[(T_1 - T_2)/r]\,(\mathrm{d}r/\mathrm{d}\eta). \tag{II-16}$$

Similar application of the chain rule to Eqs. II-9 and II-10 gives

$$\mathrm{d}\kappa_2/\mathrm{d}\eta = [(\kappa_1 - \kappa_2)/r]\,(\mathrm{d}r/\mathrm{d}\eta) \tag{II-17}$$

and

$$(\mathrm{d}r/\mathrm{d}\eta) = \lambda_1(1 - \kappa_2^2 r^2)^{1/2}. \tag{II-18}$$

Eqs. II-8, II-15, II-11, and II-12 are put in the proper form by differentiating them with respect to η and rearranging terms to give

$$\frac{\mathrm{d}\kappa_1}{\mathrm{d}\eta} = -\frac{1}{T_1}\left[\kappa_1\frac{\mathrm{d}T_1}{\mathrm{d}\eta} + T_2\frac{\mathrm{d}\kappa_2}{\mathrm{d}\eta} + \kappa_2\frac{\mathrm{d}T_2}{\mathrm{d}\eta}\right] \tag{II-19}$$

$$\frac{\mathrm{d}\lambda_2}{\mathrm{d}\eta} = \frac{1}{\rho}\left[\frac{\mathrm{d}r}{\mathrm{d}\eta} - \lambda_2\frac{\mathrm{d}\rho}{\mathrm{d}\eta}\right] \tag{II-20}$$

$$\frac{d\lambda_1}{d\eta} = \frac{(dT_1/d\eta)/(\mu_p h_0) - [-\lambda_1^{k_p+1}\lambda_3^2 + (k_p+1)\lambda_1\lambda_3^{k_p+2}](d\lambda_2/d\eta)}{(\mu_p h_0)[(k_p-1)\lambda_1^{k_p-1}\lambda_3 + (k_p+1)\lambda_3^{k_p+2}\lambda_2]} \tag{II-21}$$

$$\frac{dT_2}{d\eta} = (\mu_p h_0)\lambda_3\left\{[(k_p+1)\lambda_2\lambda_3^{k_p+1} + \lambda_3\lambda_2^{k_p+1}]\frac{d\lambda_1}{d\eta} + [(k_p-1)\lambda_2^{k_p-1} + (k_p+1)\lambda_1\lambda_3^{k_p+1}]\frac{d\lambda_2}{d\eta}\right\} \tag{II-22}$$

Now the complete set of equations is

$$\lambda_3 = 1/(\lambda_1\lambda_2) \tag{II-23}$$

$$r = \lambda_2\rho \tag{II-24}$$

$$dr/d\eta = \lambda_1(1 - \kappa_2^2 r^2)^{1/2} \tag{II-25}$$

$$d\lambda_2/d\eta = (1/\rho)[dr/d\eta - \lambda_2\, d\rho/d\eta] \tag{II-26}$$

$$d\kappa_2/d\eta = [(\kappa_1 - \kappa_2)/r](dr/d\eta) \tag{II-27}$$

$$dT_1/d\eta = -[(T_1 - T_2)/r](dr/d\eta) \tag{II-28}$$

$$\frac{d\lambda_1}{d\eta} = \frac{(dT_1/d\eta)/(\mu_p h_0) - [-\lambda_1^{k_p+1}\lambda_3^2 + (k_p+1)\lambda_1\lambda_3^{k_p+2}](d\lambda_2/d\eta)}{[(k_p-1)\lambda_1^{k_p-1}\lambda_3 + (k_p+1)\lambda_3^{k_p+2}\lambda_2]} \tag{II-29}$$

$$\frac{dT_2}{d\eta} = (\mu_p h_0)\lambda_3\left\{[(k_p+1)\lambda_2\lambda_3^{k_p+1} + \lambda_3\lambda_2^{k_p+1}]\frac{d\lambda_1}{d\eta} + [(k_p-1)\lambda_2^{k_p-1} + (k_p+1)\lambda_1\lambda_3^{k_p+1}]\frac{d\lambda_2}{d\eta}\right\} \tag{II-30}$$

$$\frac{d\kappa_1}{d\eta} = -\frac{1}{T_1}\left[\kappa_1\frac{dT_1}{d\eta} + T_2\frac{d\kappa_2}{d\eta} + \kappa_2\frac{dT_2}{d\eta}\right] \tag{II-31}$$

These equations differ somewhat from those given by Green and Adkins, who were concerned specifically with an initially flat rubber membrane. In an initially flat membrane, the undeformed radius, ρ, is identically equal to the undeformed arc length, η, so that all the derivatives with respect to η in the above equations appear with respect to ρ in Green and Adkins. In addition, $d\rho/d\eta = 1$ in Eq. II-26 for the initially flat membrane. The corresponding expressions to Eqs. II-29 and II-30 in Green and Adkins differ since they are based on a different constitutive relation, that of the Mooney material, which is essentially a two-term Ogden material, with $\Phi = \mu_m[(\lambda_1^2 + \lambda_2^2 + \lambda_3^2 - 3)/2 - \Gamma(\lambda_1^{-2} + \lambda_2^{-2} + \lambda_3^{-2} - 3)/2)]$. However, if $\Gamma = 0$, the forms in Green and Adkins are identical to Eqs. II-29 and II-30 for $k_p = 2$.

At this point it should be noted that the description of the geometry of the undeformed shell is entirely contained in Eq. II-26 through $\rho(\eta)$ and $d\rho/d\eta$.

The boundary condition is that at η_b, the edge of the undeformed membrane, $\lambda_2(\eta_b) = 1$. The membrane is constrained at its edge by the hole in the plane so that no hoop stretch occurs. This means, therefore, that the initial values of extension and curvature at the apex must be properly chosen such that at the completion of numerical integration, the boundary condition is satisfied. Actually, there are only two arbitrary initial conditions at the apex, λ and κ, since $\lambda_1 = \lambda_2 = \lambda$ and $\kappa_1 = \kappa_2 = \kappa$ at the apex. Since λ is a measure of the degree of inflation, it will be considered as a parameter of the problem; this information leaves κ as the initial condition that must be chosen to correctly satisfy the boundary condition.

This work was supported in part by grants HL21425 and HL11414 from the National Heart and Lung Institute and RR-01032 from the General Clinical Research Centers Program of the Division of Research Resources, National Institutes of Health, Bethesda, Maryland. Data organization and analysis were performed in part on the PROPHET System, a national computer resource sponsored by the Chemical/Biological Information Handling Program, National Institutes of Health.

Received for publication 30 October 1978 and in revised form 9 February 1979.

REFERENCES

ALEXANDER, H. 1971. Tensile instability of initially spherical balloons. *Int. J. Eng. Sci.* **9**:151–162.

BOGEN, D. 1977. The mechanical disadvantage of myocardial infarction: a model of the infarcted ventricle. Ph.D. Thesis. Harvard University, Cambridge.

GREEN, A. E., and J. E. ADKINS. 1960. Large Elastic Deformations. Oxford University Press, London. 138–160.

GRIMM, A. F., K. V. KATELE, R. KUBOTA, and W. V. WHITEHORN. 1970. Relation of sarcomere length and muscle length in resting myocardium. *Am. J. Physiol.* **218**:1412–1416.

JANZ, R. F., and R. J. WALDRON. 1978. Predicted effect of chronic apical aneurysms on the passive stiffness of the human left ventricle. *Circ. Res.* **42**:255–263.

LAIRD, J. D. 1976. Asymptotic slope of log pressure vs. log volume as an approximate index of the diastolic elastic properties of the myocardium in man. *Circulation.* **53**:443–449.

LOWE, T. E., and E. R. LOVE. 1948. Cardiac aneurysms: A mechanical analysis of their formation. *Aust. J. Exp. Biol. Med. Sci.* **26**:497–513.

ODGEN, R. W. 1972. Large deformation isotropic elasticity—on the correlation of theory and experiment for incompressible rubberlike solids. *Proc. R. Soc. Lond. A. Math. Phys. Sci.* **326**:526–584.

SPOTNITZ, H. M., E. H. SONNENBLICK, and D. SPIRO. 1966. Relation of ultrastructure to function in the intact heart: Sarcomere structure relative to pressure volume curves of intact left ventricles of dogs. *Circ. Res.* **18**:49–66.

TRELOAR, L. R. G. 1975. The Physics of Rubber Elasticity. 3rd edition. Oxford University Press, London. 60–64.

WU, C. H. 1972. Spherelike deformations of a balloon. *Q. J. Appl. Math.* **30**:183–194.

WU, C. H., and D. Y. P. PERNG. 1972. On the asymptotically spherical deformations of arbitrary membranes of revolution fixed along an edge and inflated by large pressures—a nonlinear boundary layer phenomenon. *SIAM J. Appl. Math.* **23**:133–152.